Origin of superconductivity in layered centrosymmetric $LaNiGa_2$

H. M. Tütüncü[1] and G. P. Srivastava[2]
[1]Sakarya Üniversitesi, Fen-Edebiyat Fakültesi, Fizik Bölümü, 54187 Adapazarı, Turkey
[2]School of Physics, University of Exeter, Stocker Road, Exeter EX4 4QL, United Kingdom

(Received 15 December 2013; accepted 3 January 2014; published online 17 January 2014)

We have examined the origin of superconductivity in layered centrosymmetric $LaNiGa_2$ by employing a linear response approach based on the density functional perturbation theory. Our results indicate that this material is a conventional electron-phonon superconductor with intermediate level of coupling strength, with the electron-phonon coupling parameter of 0.70, and the superconducting critical temperature of 1.90 K in excellent accordance with experimental value of 1.97 K. The largest contribution to the electron-phonon coupling comes from the La d and Ga p electrons near the Fermi energy and the B_{3g} phonon branch resulting from vibrations of these atoms along the Γ-Z symmetry line in the Brillouin zone. © *2014 AIP Publishing LLC*. [http://dx.doi.org/10.1063/1.4862329]

Recently, superconductivity has been discovered in a number of materials which include Ni atoms in their unit cells.[1–10] This discovery is a surprise, as due to the high Ni content in these materials a ferromagnetic ground state would have been expected rather than a superconducting state. The centrosymmetric intermetallic superconductor $LaNiGa_2$ is one of these materials. This material is the first nickel-based ternary-gallide superconductor. The first experimental study on this material was made by Romaka and coworkers,[11] who measured the lattice parameters. Following this experimental work, Aoki and coworkers[1] measured the electrical resistivity, thermoelectric power, Hall coefficient, magnetic susceptibility, magnetization M, and specific heat of polycrystalline samples. Moreover, they mentioned that $LaNiGa_2$ shows a bulk superconductivity with the transition temperature of 2.0 K. Subsequently, superconductivity with $T_C = 1.97$ K in this Ni-based ternary compound was measured by dc susceptibility and heat-capacity techniques.[4] Very recently, using muon spin rotation and relaxation experiments, Hillier and coworkers[9] have concluded that this material is characterised with weak spin-orbit coupling.

Although there is wealth of experimental works presented in recent years on structural and superconducting properties of the layered centrosymmetric superconductor $LaNiGa_2$, less attention has been paid on the theoretical side. The electronic structure is calculated by the full-potential augmented plane-wave method.[12] The electronic structure and fermiology of this material have been detailed by Singh.[13] This theoretical work, based on the generalized gradient approximation of Perdew, Burke, and Ernzerhof (PBE),[14] showed that $LaNiGa_2$ has a complex three-dimensional Fermi surface, derived mainly from Ga p states that hybridize with Ni d states. Comparing with experimental specific heat data, Singh[13] inferred a weakly coupled superconducting state. However, the origin of the development of superconductivity in this material remains elusive.

In this Letter, we present results of a systematic and detailed first-principles study of the electronic, vibrational, and superconducting properties of $LaNiGa_2$. Having verified the electronic structure results of Ref. 13, we identify the dominant phonon modes and the high density electron states that are involved in determining superconductivity in this material.

$LaNiGa_2$ possesses the base-centered orthorhombic (bco) structure, with space group Cmmm (D_{2h}). There are two formula units in the unit cell,[9,13] and the atoms fill the following Wyckoff positions: La in the position 4j (0, y^{La}, 0), Ni in the position 4i (0, y^{Ni}, 0), and Ga atoms in positions (4i) (0, y^{Ga}, 0), (2d) (0, 0, 0.5) and (2b) (0.5, 0, 0). The experimental lattice parameters,[11] $a = 4.29$ Å, $b = 17.83$ Å, and $c = 4.273$ Å are used as input data in our calculations, while equilibrium internal coordinates (y^{La}, y^{Ni}, and y^{Ga}) are obtained by the total energy minimization procedure. Our calculations employ density functional theory, within the generalized gradient approximation (GGA) as exercised in the Quantum-ESPRESSO package.[15] The electronic exchange-correlation energy is treated in the scheme of PBE.[14] Ultrasoft pseudopotentials[16,17] are used for interactions between ions and electrons. A basis set containing all plane waves up to the cut-off energy of 60 Ry has been chosen. The Brillouin zone is sampled using the Monkhorst-Pack scheme with $(24 \times 24 \times 24)$ **k** points for the electronic properties and a $(8 \times 8 \times 8)$ **q** mesh has been used for phonon calculations. Dynamical matrices have been computed on a $(2 \times 2 \times 2)$ **q**-point mesh, and a Fourier interpolation has been made to obtain phonon frequencies for any chosen **q** point. Fermi-surface sampling for the evaluation of the electron-phonon matrix elements was done using the $(24 \times 24 \times 24)$ **k** mesh with the Gaussian parameter width $\sigma = 0.03$ Ry. The technique for the calculation of the electron-phonon coupling has been described clearly in our previous works.[18,19]

Our calculated internal coordinates $y^{La} = 0.3589$, $y^{Ni} = 0.0714$, and $y^{Ga} = 0.2087$ are in good accordance with the previous GGA values[13] of 0.3591, 0.0719, and 0.2092, respectively. An analysis of the electronic structure shows that both electron and hole bands cross the Fermi level, clearly indicating the metallic nature. The total and atom projected electronic density of states (eDOS) are presented in Fig. 1. The La 5s, Ga 4p, and Ni 3d states are strongly hybridized in the region between −1 eV and the Fermi level. The Fermi level is situated at the decreasing part of a small peak at −0.3 eV. The orbital analysis of the DOS indicates

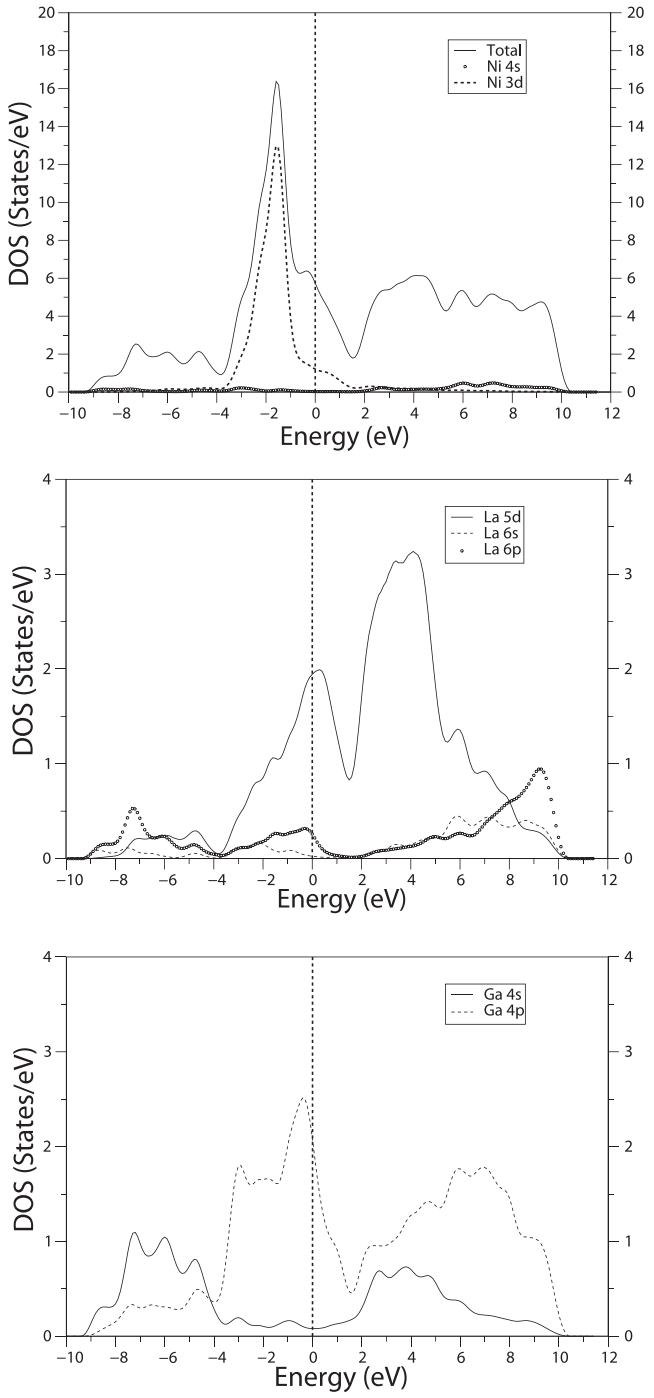

FIG. 1. Top panel: total electronic density of states. Middle and bottom panels: local density of states, calculated by projecting wavefunctions onto orthogonalised atomic wavefunctions in the subspace spanned by the atomic basis.

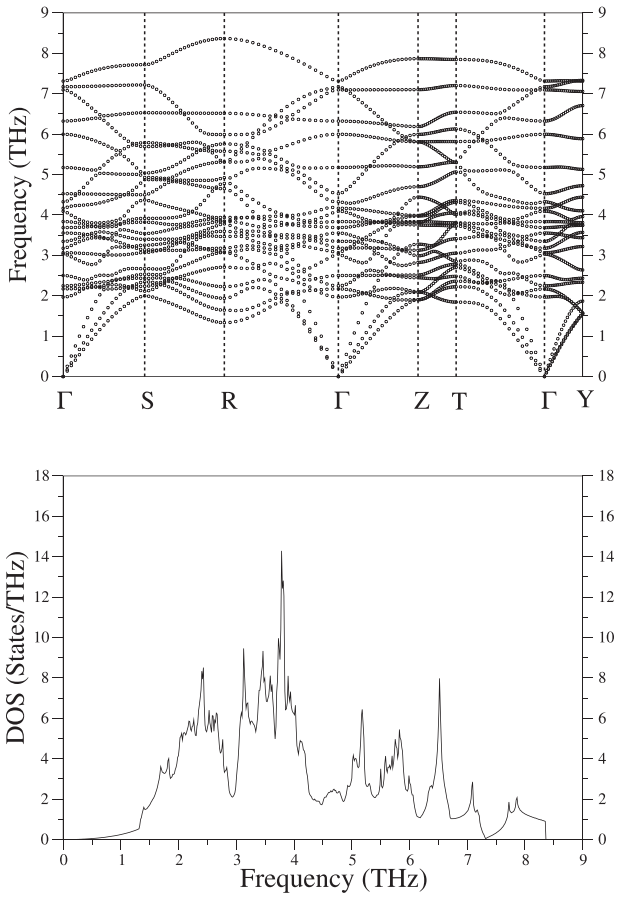

FIG. 2. (a) Phonon dispersion curves, and (b) phonon density of states for the layered centrosymmetric superconductor $LaNiGa_2$.

that mainly La 5d, Ga 4p, and Ni 3d states are contributing to the total values of DOS at the Fermi level ($N(E_F)$). The value of $N(E_F)$ is found to be 5.64 states/eV. The contributions of La, Ga, and Ni electronic states to $N(E_F)$ are as much as 40.4%, 38.6%, and 21%, respectively. In particular, the La 5d, Ga 4p, and Ni 3d states contribute 33%, 36%, and 20%, respectively. Thus, one can conclude that the electronic properties of $LaNiGa_2$ are greatly influenced by the La 5d, Ga 4p, and Ni 3d electronic states.

The calculated phonon dispersion curves along the high symmetry lines in the Brillouin zone and the phonon density of states (pDOS $F(\omega)$) for $LaNiGa_2$ are displayed in Fig. 2. Factor group analysis at the zone-center generates 21 optical modes: 9 Raman active modes of $3A_g + 3B_{3g} + 3B_{1g}$ and 12 infrared active modes of $4B_{1u} + 4B_{2u} + 4B_{3u}$. The calculated zone-center frequencies and the dominant ions in contribution to the eigenvectors of the vibrational modes are listed in Table I. The calculated vibration at 1.97 THz with B_{3u} symmetry is characterized by the vibrations of all atoms in the unit cell with the maximum contribution coming from Ni atoms. The second optical vibration (B_{3g}) at 2.17 THz is polarized along the $\hat{z}$ axis with a stationary Ni atom. All atoms in the unit cell contribute to the intermediate B_{1u} vibration with the minimum contribution coming from La atoms. The B_{1g} mode at 2.50 THz is polarized along the $\hat{x}$ axis with the vibrations of La and Ga atoms. Ni and Ga atoms are static for the A_g phonon mode at 3.03 THz, while La atoms vibrate against each other along the $\hat{y}$ direction. The B_{1u} mode at 3.06 THz involves the motions of all atoms in the unit cell along the [001] direction. The second B_{3u} phonon mode is totally generated by the lighter Ga and Ni atoms with La atoms rest. The vibrations of Ga, Ni, and La atoms create the phonon mode at 3.35 THz with B_{2u} symmetry. The B_{3g} phonon mode at 3.55 THz includes atomic vibrations from Ga and La atoms with maximum contribution coming from Ga atoms due to the lighter mass of Ga atoms compared to the heavy mass of La atoms. We have observed an infrared active phonon mode at 3.69 THz with B_{1u} symmetry which is created by the vibrations of all atoms

TABLE I. Calculated phonon modes (in THz) and electron-phonon coupling parameters at the zone-center for $LaNiGa_2$. Factor group analysis at the zone-center generates 21 optical modes: 9 Raman active modes of $3A_g + 3B_{3g} + 3B_{1g}$ and 12 infrared active modes of $4B_{1u} + 4B_{2u} + 4B_{3u}$. Mode activity (R = Raman, IR = Infrared).

Symmetry	Mode activity	Frequency	Involved atoms	λ
B_{3u}	IR	1.967	Ni + Ga + La	0.019
B_{3g}	R	2.169	Ga + La	0.036
B_{1u}	IR	2.245	Ga + Ni + La	0.017
B_{1g}	R	2.500	La + Ga	0.046
A_g	R	3.030	La	0.134
B_{1u}	IR	3.063	Ga + La + Ni	0.027
B_{3u}	IR	3.176	Ga + Ni	0.008
B_{2u}	IR	3.345	Ga + Ni + La	0.021
B_{3g}	R	3.552	Ga + La	0.031
B_{1u}	IR	3.686	Ga + La + Ni	0.004
B_{3u}	IR	3.836	Ga + La	0.006
B_{2u}	IR	4.091	Ga	0.020
B_{1g}	R	4.165	Ni	0.054
B_{2u}	IR	4.325	Ga + La + Ni	0.001
B_{3g}	R	4.524	Ni	0.036
A_g	R	5.173	Ga + Ni	0.070
B_{1g}	R	5.996	Ga	0.026
B_{2u}	IR	6.322	Ga + Ni	0.003
B_{3u}	IR	7.095	Ni + Ga	0.001
B_{1u}	IR	7.172	Ni + Ga	0.001
A_g	R	7.312	Ni + Ga	0.054

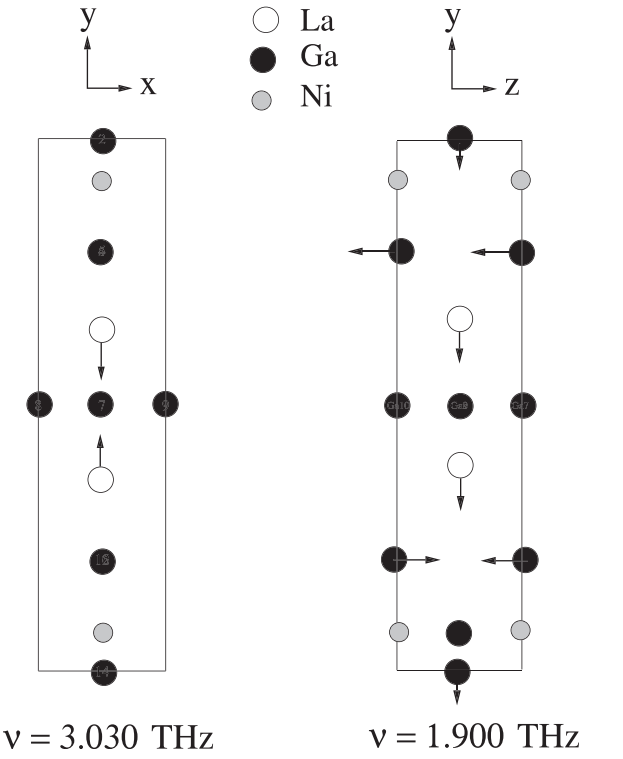

FIG. 3. Eigenvectors representation of the A_g phonon mode at 3.030 THz (left panel) and the B_{3g} phonon mode at 1.900 THz (right panel) for $LaNiGa_2$.

in the unit cell. Ga and La atoms vibrate for phonon mode at 3.84 THz with B_{3u}, while Ni atoms are static. Only Ga atoms make contributions to the B_{2u} phonon mode at 4.09 THz, while the B_{1g} phonon mode with the frequency of 4.165 is totally dominated by the vibration of Ni atoms with Ga and La atoms rest. All atoms in the unit cell vibrate for the phonon mode at 4.33 THz with B_{2u} symmetry but the maximum contribution from Ga atoms. The opposing vibrations of Ni atoms along the [001] direction generates the phonon mode at 4.52 THz with B_{2g} symmetry. The Raman active phonon mode at 5.17 THz has A_g symmetry with the vibrations of Ga and Ni atoms, while La atoms are static. Only Ga atoms vibrate for the B_{1g} phonon mode with the frequency of 6.00 THz. A mixture of vibrations of Ga and Ni atoms characterize the phonon modes above 6 THz, with La atoms at rest.

Table I also presents the calculated electron-phonon coupling parameters of the zone-center phonon modes. All phonon modes have very small electron-phonon coupling parameters expect the phonon mode at 3.03 THz with A_g symmetry. Eigenvectors representation of this phonon mode has been pictured in Fig. 3. As can be seen from this figure, large vibrational amplitudes along [010] cause big changes in the overlap of d and p orbitals between neighbouring La and Ga atoms and thus lead to the largest electron-phonon coupling parameter with the value of 0.13 for this phonon mode at the Γ point. From our electron-phonon interaction calculations, we have observed that the electron-phonon coupling parameters of zone boundary phonon modes are larger than those of zone-center phonon modes. In order to show this clearly, we have plotted the low-lying phonon branches and their electron-phonon coupling parameters along the Γ-Z direction in Fig. 4. The most notable feature of this figure is the dispersion of B_{3g} phonon branch along this symmetry direction. Away from the zone-center, this phonon branch crosses the B_{3u} phonon branch. Then, this phonon branch crosses the longitudinal acoustic (LA) as well as the transverse acoustic (TA) branches. Due to a pronounced anomaly in the dispersion of the B_{3g} phonon branch, the electron-phonon coupling parameter of this phonon branch increases rapidly with increasing **q** wave vector. We have to mention that Ni atoms are static for this phonon mode while La and Ga atoms vibrate. At the zone boundary along [001] (the Z point), the frequency and electron-phonon coupling parameter of this phonon branch reach the values of 1.90 THz and 0.34, respectively. We have plotted the atomic displacement for this zone boundary phonon mode in Fig. 3. The vibrations of La and Ga atoms for this mode promote overlap between the La d and Ga p electronic orbitals.

In order to better understand the source of superconductivity in this material, we have plotted the Eliashberg function $\alpha^2F(\omega)$ and the electron-phonon coupling parameter λ in Fig. 5. The difference between the shapes of the $\alpha^2F(\omega)$ and $F(\omega)$ indicates that all phonon modes make different contributions to the electron-phonon interaction. The electron-phonon coupling parameter λ represents the magnitude of correction of several important physical properties due to the electron-phonon many-body interaction, such as quasi particle energy, electronic heat capacity, and effective mass. Figure 5 shows that phonon modes below 4 THz due to the vibrations of La and Ga atoms contribute about 85% towards λ. This is acceptable, as the states near the Fermi energy are dominated by La d and Ga p characters. The larger contribution from low frequency phonons is due to the factor of $\frac{1}{\omega}$ in λ which is given by

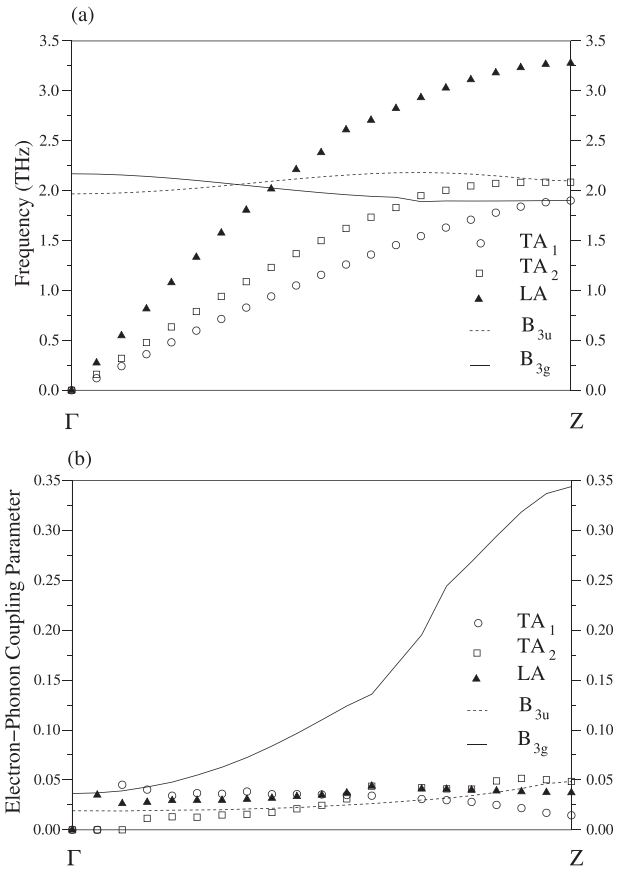

FIG. 4. (a) The TA_1, TA_2, LA, B_{3u}, and B_{3g} branches of $LaNiGa_2$ along the Γ-Z direction. (b) The calculated electron-phonon coupling parameters of these phonon branches along the [001] symmetry direction.

$$\lambda = 2\int \frac{\alpha^2 F(\omega)}{\omega} d\omega. \tag{1}$$

The average electron-phonon coupling parameter is found to be $\lambda = 0.70$ which shows that the electron-phonon interaction in this material is medium. To obtain the superconductor transition temperature (T_C), we have used the Allen-Dynes equation

$$T_C = \frac{\omega_{\ln}}{1.2}\exp\left(-\frac{1.04(1+\lambda)}{\lambda - \mu^*(1+0.62\lambda)}\right), \tag{2}$$

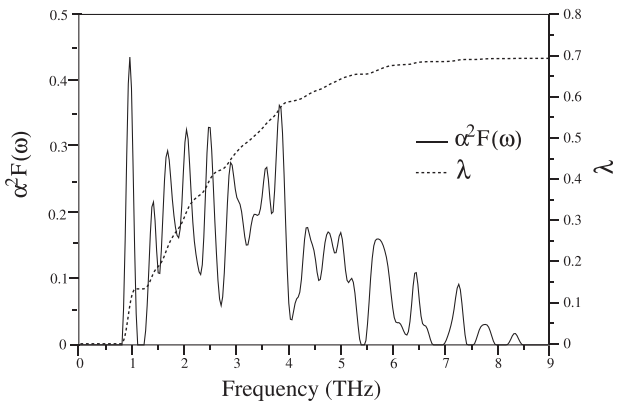

FIG. 5. The calculated electron-phonon spectral function $\alpha^2F(\omega)$ (left axis) and the variation of the electron-phonon coupling parameter (right axis) with increasing frequency $\lambda(\omega)$.

which links the value of T_C with the electron-phonon coupling parameter λ, the logarithmically averaged frequency ω_{ln}, and Coulomb repulsion μ^*. The values of ω_{ln} and Coulomb repulsion μ^*[20] can be obtained as

$$\omega_{ln} = \exp\left(2\lambda^{-1}\int_0^\infty \frac{d\omega}{\omega}\alpha^2 F(\omega) ln\omega\right), \tag{3}$$

$$\mu^* = \frac{0.20N(E_F)}{(1+N(E_F))}. \tag{4}$$

From above equations, the values of ω_{ln} and μ^* are calculated to be 111.52 K and 0.17, respectively. This estimated value of μ^* lies in the acceptable range of 0.10 and 0.20. Inserting the calculated values of λ, ω_{ln}, and μ^* into the Allen-Dynes formula, the value of T_C is found to be 1.90 K, which is in excellent agreement with the experimental values[1,4] of 2.01 and 1.97 K. Thus, we can conclude that the conventional electron-phonon-coupling picture explains the superconductivity of $LaNiGa_2$.

The recent experimental work of Hiller and coworkes[9] showed that the spin-orbit coupling interaction is weak in $LaNiGa_2$. The observation of weak spin-orbit interaction suggests that dominant states at or near E_F are mainly s-type, thus contradicting the μSR measurements that might indicate an unconventional triplet superconductor. This is verified from the analysis of the band structure in this work as well as in Ref. 13. There is further support for s-type superconductivity in this material as there is excellent agreement for T_C between experimentally reported value[1] and our calculated value without considering spin-orbit coupling interaction.

In conclusion, we have found that while the states near the Fermi-level are dominated by La 5d, Ga 4p, and Ni 3d electronic states, low frequency (below 4 THz) phonons are contributed by La and Ga vibrations and high frequency(above 4 THz) phonons are contributed by Ni and Ga atoms. The difference between the shapes of the $\alpha^2F(\omega)$ and $F(\omega)$ functions indicates that electrons couple more strongly with lower frequency phonons (below 4 THz). The large vibrational amplitudes of La and Ga atoms promote overlap between the d and p electron orbitals of these atoms and thus give rise to a substantial contribution towards the electron-phonon coupling parameter λ. The average electron-phonon coupling parameter λ is found to be 0.70, and the superconducting critical temperature is calculated to be 1.90 K, in good agreement with the experimental value of around 1.97 K.

The calculations were performed using the Intel Nehalem (i7) cluster (ceres) at the University of Exeter.

[1]Y. Aoki, K. Terayama, and H. Sato, J. Phys. Soc. Jpn. **64**, 3986 (1995).
[2]V. K. Pecharsky, L. L. Miller, and K. A. Gschneidner, Jr., Phys. Rev. B **58**, 497 (1998).
[3]T. He, Q. Huang, A. P. Ramirez, Y. Wang, K. A. Regan, N. Rogado, M. A. Hayward, M. K. Haas, J. S. Slusky, K. Inumaru, H. W. Zandbergen, N. P. Ong, and R. J. Cava, Nature (London) **411**, 54 (2001).
[4]N. L. Zeng and W. H. Lee, Phys. Rev. B **66**, 092503 (2002).
[5]M. Uehara, T. Yamazaki, T. Kori, T. Kashida, Y. Kimishima, and I. Hase, J. Phys. Soc. Jpn. **76**, 034714 (2007).

[6]M. Uehara, A. Uehara, K. Kozawa, and Y. Kimishima, J. Phys. Soc. Jpn. **78**, 33702 (2009).
[7]A. D. Hillier, J. Quintanilla, and R. Cywinski, Phys. Rev. Lett. **102**, 117007 (2009).
[8]J. Quintanilla, A. D. Hillier, J. F. Annett, and R. Cywinski, Phys. Rev. B **82**, 174511 (2010).
[9]A. D. Hillier, J. Quintanilla, B. Mazidian, J. F. Annett, and R. Cywinski, Phys. Rev. Lett. **109**, 097001 (2012).
[10]R. T. Gordon, N. D. Zhigadlo, S. Weyeneth, S. Katrych, and R. Prozorov, Phys. Rev. B **87**, 094520 (2013).
[11]V. A. Romaka, Y. N. Grin, Y. P. Yarmolyuk, R. V. Skolozdra, and A. A. Yartys, Ukr. Fiz. Zh. **28**, 227 (1983).
[12]I. Hase and T. Yanagisawa, J. Phys. Soc. Jpn. **81**, 103704 (2012).
[13]D. J. Singh, Phys. Rev. B **86**, 174507 (2012).
[14]J. P. Perdew, K. Burke, and M. Ernzerhof, Phys. Rev. Lett. **77**, 3865 (1996).
[15]P. Giannozzi, S. Baroni, N. Bonini, M. Calandra, R. Car, C. Cavazzoni, D. Ceresoli, G. L. Chiarotti, M. Cococcioni, I. Dabo, A. D. Corso, S. de Gironcoli, S. Fabris, G. Fratesi, R. Gebauer, U. Gerstmann, C. Gougoussis, A. Kokalj, M. Lazzeri, L. Martin-Samos, N. Marzari, F. Mauri, R. Mazzarello, S. Paolini, A. Pasquarello, L. Paulatto, C. Sbraccia, S. Scandolo, G. Sclauzero, A. P. Seitsonen, A. Smogunov, P. Umari, and R. M. Wentzcovitch, J. Phys.: Condens. Matter **21**, 395502 (2009).
[16]D. Vanderbilt, Phys. Rev. B **41**, 7892 (1990).
[17]A. M. Rappe, K. M. Rabe, E. Kaxiras, and J. D. Joannopoulos, Phys. Rev. B **41**, 1227 (1990).
[18]H. M. Tütüncü and G. P. Srivastava, J. Phys.: Condens. Matter **18**, 11089 (2006).
[19]H. M. Tütüncü, S. Bağcı, and G. P. Srivastava, Phys. Rev. B **82**, 214510 (2010).
[20]K. Bennemann and J. Garland, *in Superconductivity in d- and f-Band Metals*, edited by D. H. Douglass (Plenum, New York, 1973), p. 103.